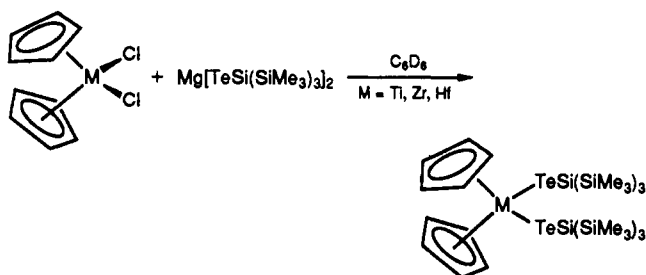


Figure 1. ORTEP view of $\text{Mg}[\text{TeSi}(\text{SiMe}_3)_3]_2(\text{THF})_2$ with thermal ellipsoids at 50% probability.

400-MHz ^1H NMR spectrum shows a singlet for the sitels and a complex AA'BB' pattern at 3.92 ppm for the ethylene groups of the 12-crown-4 ligands.

All of the group 2 telluroate derivatives act as clean sources of the sitel ligand in metathesis reactions with metal halides. An illustrative example that leads to the formation of early transition metal-telluroate compounds⁶ cleanly and in high yield is shown below; further details will be described in a full account.



The X-ray structure of $\text{Mg}[\text{TeSi}(\text{SiMe}_3)_3]_2(\text{THF})_2$ shows the magnesium atom surrounded in a distorted tetrahedral fashion by two THF oxygens and two telluriums from the sitel ligands (Figure 1).¹³ The Mg-Te bond lengths are virtually equal (2.720, 2.714 (1) Å) and are as predicted on the basis of ionic radii (Mg^{2+} , 0.71 Å; Te^{2-} , 2.07 Å¹¹). The bulk of the sitel ligands is no doubt responsible for the large Te-Mg-Te angle of 135.48 (4)° and the rather acute O-Mg-O angle of 94.8 (1)°. The Te-Mg-O angles are not equal, so that for each of the two tellurium atoms there is one large (111.77, 114.37 (7)°) and one small angle (96.37, 94.79 (7)°). This difference may be attributed to steric repulsion from the tellurium sp^3 lone pairs, since the smaller angle appears when the THF oxygen is trans to the Te-Si vector in the sitel ligand, but packing effects cannot be excluded.

$\text{Ca}[\text{TeSi}(\text{SiMe}_3)_3]_2(\text{THF})_4$ crystallizes with four THFs and features a highly distorted octahedral coordination sphere about calcium.¹³ Figure 2 shows an ORTEP view of the molecule illustrating the disordered THF. The molecule has strict inversion symmetry with the calcium atom located at the origin of the cell, resulting in angles of 180° for all three trans interactions. Inspection of the angles between cis coordination sites highlights the extent to which the molecule is distorted. These angles, which

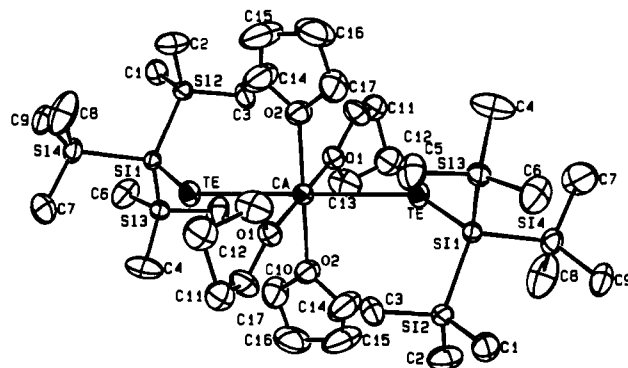


Figure 2. ORTEP view of $\text{Ca}[\text{TeSi}(\text{SiMe}_3)_3]_2(\text{THF})_4$ with thermal ellipsoids at 50% probability.

range from 77.33 (5)° to 92.73 (9)°, appear to result from interligand repulsions. The predicted Ca-Te bond length of 3.21 Å¹¹ is close to the experimentally determined value of 3.197 (1) Å.

In summary, we have prepared and fully characterized the first examples of isolable telluroate derivatives of group 2. Preliminary results indicate that they function as useful telluroating synthons; further structural and reactivity studies are in progress.

Acknowledgment. We are grateful to the National Science Foundation (CHE-9019675) for support.

Supplementary Material Available: Details of the structure determination including tables of crystal and data collection parameters, temperature factor expressions, positional parameters, and intramolecular distances and angles (17 pages); listings of observed and calculated structure factors (75 pages). Ordering information is given on any current masthead page.

Microscopic Basis of Wetting: An in Situ Study of the Interaction between Liquids and an Organic Monolayer[†]

T. Hui Ong, Robert N. Ward, and Paul B. Davies*

Department of Chemistry, University of Cambridge
Lensfield Road, Cambridge CB2 1EW, U.K.

Colin D. Bain*

Physical Chemistry Laboratory, University of Oxford
South Parks Road, Oxford OX1 3QZ, U.K.

Received April 15, 1992

Many macroscopic properties of materials, such as wettability and adhesive strength, are governed by microscopic interfacial interactions between two condensed phases. Direct investigation of such interfaces is difficult, as they are not readily accessible to conventional surface probes. Here we report the use of an in situ technique, sum-frequency vibrational spectroscopy, to study how three liquids—hexane, acetonitrile, and water—interact with a model organic surface: a self-assembled monolayer of 16-methoxyhexadecanethiol ($\text{CH}_3\text{O}(\text{CH}_2)_{16}\text{SH}$, MeOHT)¹ adsorbed on gold.²

Sum-frequency spectroscopy (SFS)³ is a nonlinear optical technique in which a fixed-frequency visible laser and a tunable infrared laser are pulsed simultaneously onto an interface and light emitted at the sum frequency is detected.⁴ Analysis of SF spectra

(13) Crystal data for $\text{Te}_2\text{Si}_6\text{MgO}_2\text{C}_{26}\text{H}_{30}$: space group $\text{P}\bar{1}$ with $a = 12.033$ (2), $b = 12.650$ (2), $c = 16.757$ (3) Å, $\alpha = 98.88$ (2), $\beta = 104.853$ (13), $\gamma = 95.166$ (15)°, $V = 2413$ Å³, $d_{\text{calcd}} = 1.26$ g cm⁻³, and $Z = 2$. Data were collected at -85 °C with Mo K α ($\lambda = 0.7107$ Å) radiation. A total of 6281 unique data were collected. The structure was solved by Patterson methods and refined by least-squares and Fourier techniques using 353 variables against 5519 data, for which $F^2 > 3\sigma(F^2)$, to give $R = 2.54\%$, $R_w = 3.29\%$, and GOF = 1.60. Crystal data for $\text{Te}_2\text{CaSi}_6\text{O}_4\text{C}_{34}\text{H}_{36}$: space group $\text{P}\bar{1}$ with $a = 9.965$ (2), $b = 13.822$ (3), $c = 10.434$ (2) Å, $\alpha = 87.157$ (15), $\beta = 86.013$ (14), $\gamma = 89.968$ (18)°, $V = 1432$ Å³, $d_{\text{calcd}} = 1.25$ g cm⁻³, and $Z = 1$. Data were collected at -88 °C with Mo K α ($\lambda = 0.7107$ Å) radiation. A total of 6549 unique data were collected. The structure was solved by Patterson methods and refined by least-squares and Fourier techniques using 222 variables against 5377 data, for which $F^2 > 3\sigma(F^2)$, to give $R = 3.32\%$, $R_w = 4.39\%$, and GOF = 1.92. The crystal structures were determined by Dr. F. J. Hollander at the University of California—Berkeley X-ray facility (CHEXRAY).

[†] This work was supported by the SERC, Unilever Research (Port Sunlight Laboratory), and the Royal Society. T.H.O. acknowledges a scholarship from the Public Service Commission of Singapore.

(1) MeOHT was synthesized according to published procedures (ref 2) and was pure by ^1H NMR analysis, mp 30–31 °C (lit. mp 29.5–30.5 °C).

(2) Bain, C. D.; Whitesides, G. M. *J. Am. Chem. Soc.* **1988**, *110*, 5897–5898.

(3) Shen, Y. R. *Nature* **1989**, *337*, 519–525.

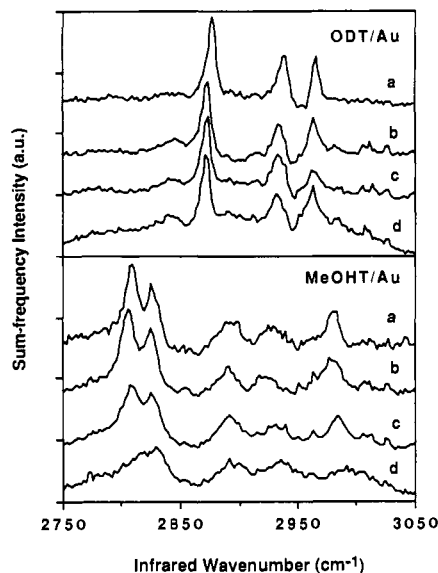


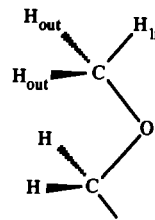
Figure 1. Infrared-visible sum-frequency spectra of monolayers of octadecanethiol, ODT (upper figure) and 16-methoxyhexadecanethiol, MeOHT (lower figure), on gold in contact with (a) air, (b) hexane- d_{14} , (c) acetonitrile- d_3 , and (d) water. Spectra are offset for ease of comparison.

can be complex, but to interpret the data presented here it is essential to understand only a few key features. First, the SF signal arises primarily from the interface and not from the liquid. Second, the SF signal is resonantly enhanced when the frequency of the infrared laser coincides with a vibrational mode that is both infrared and Raman active. Third, the intensity of the resonances depends on the orientational order of the molecules in the monolayer: the more disordered the monolayer, the weaker the SF peaks.

We seek to answer two questions: How do liquids interact with the polar oxygen atom in the methyl ether? Do these interactions perturb the structure of the monolayer? We compared the SF spectra in the C-H stretching region of a monolayer of octadecanethiol ($\text{CH}_3(\text{CH}_2)_{17}\text{SH}$, ODT), which does not contain an oxygen atom, with that of MeOHT on gold.⁵ Both molecules form monolayers that are bound to the gold substrate through the sulfur atom⁶ and are densely packed and highly oriented with an angle of $\sim 30^\circ$ between the chain axis and the normal to the surface.⁷

Figure 1 shows the SF spectra of these monolayers in contact with air, hexane- d_{14} , acetonitrile- d_3 , and water. The spectrum of ODT in air contains three principal peaks, all arising from the terminal methyl group.^{8,9} The spectrum of MeOHT shows five peaks. The doublet¹⁰ at 2810 and 2828 cm^{-1} and the singlet at

2980 cm^{-1} are assigned to A' stretching modes (principally $\text{CH}_{2(\text{out})}$ and $\text{CH}_{(\text{in})}$, respectively), and the peak at 2930 cm^{-1} is assigned to the asymmetric (A'') stretch ($\text{CH}_{2(\text{out})}$).¹¹ The remaining peak at 2890 cm^{-1} is an overtone or combination of CH_3 deformation modes.¹²



The effect of hexane- d_{14} on both monolayers is similar: the methyl resonances show small red shifts compared to air, but little other change. This similarity is not surprising since hexane interacts primarily through short-range dispersion forces and neither an oxygen atom nor a methylene group is highly polarizable.¹³

The spectrum of MeOHT under acetonitrile shows pronounced broadening of the low-frequency doublet and a blue shift of 2–5 cm^{-1} in all of the stretching modes compared with hexane. In contrast, the peak positions of ODT under hexane and acetonitrile are identical. Acetonitrile is a polar molecule which can interact with the ether oxygen atom through dipole-dipole forces. These interactions appear to lead to a general strengthening of the C-H bonds and inhomogeneous broadening of the stretching modes.

Dramatic changes occur when the monolayer of MeOHT is placed in contact with water. All five peaks broaden, the intensity of the low-frequency doublet decreases, and the frequencies of all of the C-H stretching modes increase: compared to hexane, the A'' mode (2938 cm^{-1}) is blue shifted by 8 cm^{-1} and the high-frequency A' mode (2995 cm^{-1}) by 14 cm^{-1} .¹⁴ Such spectral changes are absent in ODT where there is only a $\sim 25\%$ decrease in the intensity of the symmetric methyl stretch at 2874 cm^{-1} and a slight broadening of the other two peaks. The upward shift in the C-H stretching modes of the methyl group in MeOHT is consistent with hydrogen bonding between water molecules and the buried oxygen linkage. Spectra of dimethyl ether and its water complex in an argon matrix, recorded by Barnes,¹⁵ showed a 19 cm^{-1} shift in the A'' mode and a 12 cm^{-1} shift in the high-frequency A' mode upon complexation of the ether with water. This shift was interpreted¹⁵ in terms hydrogen bonding: the resulting reduction in electron donation from the oxygen lone pairs into the CH antibonding orbitals causes a strengthening of the C-H bonds.¹⁶ A range of hydrogen-bond geometries would lead to the observed broadening of the sum-frequency resonances. The loss of intensity in the low-frequency A' methyl mode further suggests that hydrogen bonding between the underlying oxygen atoms and water may induce increased disorder near the outer surface of the monolayer.

The molecular interactions at the solid-liquid interface inferred from these spectra correlate well with the observed macroscopic contact angles. The difference in the work of adhesion, W_{adh} , between the two monolayers and a liquid is given by $\gamma_{\text{lv}}(\cos \theta_1 - \cos \theta_2)$, where γ_{lv} is the liquid-vapor surface tension and θ_1 and θ_2 are the contact angles of the liquid on the monolayers of

(4) The IR laser pulses (2.5 mJ per pulse, ~ 4 ns, 11.5 Hz) were generated by third-order stimulated Stokes scattering of an Nd:YAG-pumped tunable dye laser in high-pressure hydrogen (Rabinowitz, P.; Perry, B. N.; Levinos, N. *IEEE J. Quantum Electron.* **1986**, *QE22*, 797–801). The second harmonic of the Nd:YAG laser served as the visible pulse. All electric fields were p-polarized.

(5) These monolayers were formed according to established procedures (ref 6). Contact angle measurements agree with those previously reported.

(6) Bain, C. D.; Troughton, E. B.; Tao, Y.-T.; Evall, J.; Whitesides, G. M.; Nuzzo, R. G. *J. Am. Chem. Soc.* **1989**, *111*, 321–335.

(7) Porter, M. D.; Bright, T. B.; Allara, D. L.; Chidsey, C. E. D. *J. Am. Chem. Soc.* **1987**, *109*, 3559–3568. Laibinis, P. E.; Whitesides, G. M.; Allara, D. L.; Tao, Y.-T.; Parikh, A. N.; Nuzzo, R. G. *J. Am. Chem. Soc.* **1991**, *113*, 7152–7167. Nuzzo, R. G. Private communication.

(8) Harris, A. L.; Chidsey, C. E. D.; Levinos, N. J.; Loiacono, D. N. *Chem. Phys. Lett.* **1987**, *141*, 350–356.

(9) The methylene modes in an all-trans hydrocarbon chain are inactive in SFS. The weak features near 2850 and 2920 cm^{-1} probably arise from gauche conformations near the methyl terminus of the chain. (Nuzzo, R. G.; Korenic, E. M.; Dubois, L. H. *J. Chem. Phys.* **1990**, *93*, 767–773; Hautman, J.; Bareman, J. P.; Mar, W.; Klein, M. L. *J. Chem. Soc., Faraday Trans.* **1991**, *87*, 2031–2037).

(10) The doublet arises from a Fermi resonance between the A' $\text{CH}_{2(\text{out})}$ mode and a combination of methyl deformation modes.

(11) The A' and A'' modes are symmetric and antisymmetric, respectively, with respect to the plane of the hydrocarbon backbone.

(12) Allan, A.; McKean, D. C.; Perchard, J.-P.; Josien, M.-L. *Spectrochim. Acta* **1971**, *27A*, 1409–1437.

(13) The ether oxygen is actually less polarizable than a methylene group, though dipole-induced dipole interactions may compensate for the weaker dispersion interactions (Hill, N. E.; Vaughan, W. E.; Price, A. H.; Davies, M. *Dielectric Properties and Molecular Behaviour*; Van Nostrand Reinhold: London, 1969).

(14) The interpretation of frequency changes in the low-frequency doublet is complicated by the Fermi resonance.

(15) Barnes, A. J.; Beech, T. R. *Chem. Phys. Lett.* **1983**, *94*, 568–570.

(16) See also: McKean, D. C.; Coats, A. M. *Spectrochim. Acta* **1989**, *45A*, 409–419. The existence of C-H...OH₂ hydrogen bonds in methyl ethers is not established (Desiraju, G. R. *Acc. Chem. Res.* **1991**, *24*, 290–296) and would lead to a decrease, not the observed increase, in C-H resonance frequencies.

MeOHT and ODT, respectively. We find values of ΔW_{adh} of 2 mJ m⁻² for hexadecane, 9 mJ m⁻² for acetonitrile, and 43 mJ m⁻² for water. For water, this corresponds to an interaction free energy of ~ 5 kJ per mole of MeOHT.

Sum-frequency spectroscopy shows that specific microscopic interactions, dependent on the chemical structure of both the liquid and the monolayer, clearly exist at the solid-liquid interface. To understand the wettability of organic surfaces, changes in the structure of the surface must be considered, particularly when hydrogen bonding is possible.

Registry No. MeOHT, 115422-11-2; Au, 7440-57-5; hexane, 110-54-3; acetonitrile, 75-05-8.

The First Catalytic Iron-Mediated [4 + 1] Cyclopentenone Assembly: Stereoselective Synthesis of 2,5-Dialkylidenecyclo-3-pentenones

Bruce E. Eaton* and Brent Rollman

Department of Chemistry
Washington State University
Pullman, Washington 99164

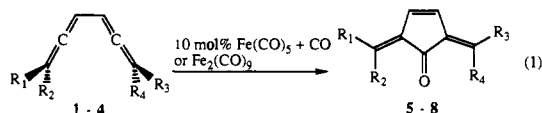
James A. Kaduk

Amoco Corporation, Naperville, Illinois 60566

Received March 4, 1992

Herein is described the first transition metal catalyzed [4 + 1] cycloaddition reaction.¹ Conjugated diallenes react with CO under mild conditions in the presence of iron carbonyls to give the new ring structure of 2,5-dialkylidenecyclo-3-pentenones² in good yield. Several examples of [4 + 1] cycloadditions have been reported recently.³ The assembly of 5-membered carbocyclic rings frequently involves [3 + 2]⁴ and Pauson-Khand⁵ [2 + 2 + 1] cobalt-mediated cycloadditions. There is no precedent for iron carbonyls catalyzing [4 + 1] cycloaddition reactions.

Our discovery of this reaction came when diallene **1**⁶ was treated with 1 equiv of Fe₂(CO)₉ at ambient temperature (eq 1), yielding **5** (79%) in less than 9 min! Surprisingly, the catalytic [4 + 1] reaction was achieved with Fe(CO)₅ (10 mol %, 17 mM CO).



- 1, 5 R₁, R₃, R₂, R₄ = CH₃
- 2, 6 R₁, R₃ = C(CH₃)₃, R₂, R₄ = CH₃
- 3, 7 R₁, R₃ = C₆H₅, R₂, R₄ = CH₃
- 4, 8 R₁, R₄ = CH₃, R₂, R₃ = C(CH₃)₃ and R₂, R₃ = CH₃, R₁, R₄ = C(CH₃)₃

Meso conjugated diallenes **2**⁷ and **3**⁸ gave a highly stereoselective reaction to form only **6** (72%) and **7** (81%), which would be difficult to prepare by other synthetic methods.

We also tested Fe₃(CO)₁₂ (10 mol %, 17 mM CO, THF) and found no detectable reaction. In contrast, Fe₂(CO)₉ (10 mol %, 17 mM CO) rapidly converted one turnover of **1** to **5**, with subsequent product formation occurring at a rate comparable to that observed for Fe(CO)₅ (Table I).

The catalytic reaction rate was measured at varying concentrations of **1**, Fe(CO)₅, and CO (Table I). It was found that the reaction was approximately inverse second order in CO and first order in **1** and Fe(CO)₅. These results are consistent with rate-determining coordination of monomeric iron to the diallene with concomitant loss of two CO groups.

The stereoselectivity of alkylidene bond formation provides information about the topology of this [4 + 1] reaction. Why was only one product formed in the case of the diallenes **2** and **3**? Since only one of the two symmetric products was formed using meso conjugated diallenes, the iron appears to exert a π -facial preference in binding or reaction with the diallene ligand. To probe reaction topology, a chiral (racemic) diallene diastereomer was studied. By fractional crystallization⁶ pure diastereomer **2** was obtained as determined by X-ray crystallography.⁶ A reaction of 4:6 mixture of diastereomers **2**(meso, C₂)/**4**(chiral, C₂) was stopped at 45% completion with 44% recovered starting material. NMR analysis revealed a symmetric product consistent with **6**⁶ (89% based on recovered starting material) and confirmed by X-ray analysis (Figure 1). In addition, a minor unsymmetric isomeric product **8** was formed (7%). The recovered diallene showed a ratio of 14:86 for **2**/**4**, indicating that the meso isomer had reacted faster than the chiral (racemic) diastereomer.

Nevertheless, the formation of **8** requires stereospecific disrotatory movement of the sp diallene carbons of **4** during the cycloaddition. Since **2** was shown to give only **6**, the product **8** came from diastereomer **4**. One plausible mechanism to account for the assembly of **8** is shown in Scheme I. The kinetic data are consistent with rate-determining associative coordination of **4** to give **11** necessitating the formation of Fe(CO)₅ as part of the catalytic cycle. The reactivity of **2** is significantly greater than that of **4**, implying η^4 -coordination to the s-cis diallene conformation as opposed to a mechanism whereby facial selectivity is determined by rate-determining η^2 -coordination.

Cobalt η^4 -bisketene⁹ and iron vinylallene¹⁰ complexes isoelectronic to **11** have been characterized by X-ray crystallography. In analogy to isolobal cobalt,¹¹ molybdenum¹² and zirconium¹³ diene complexes **11** may convert to the metallocyclopentene **12**, necessitating synchronous movement of methyl (and *tert*-butyl) on both terminal diallene carbons. Insertion of CO to give **13**

(1) Liebeskind, L. S.; Chidambaram, R. *J. Am. Chem. Soc.* **1987**, *109*, 5025.

(2) These molecules resemble the biologically active methylenomycin antibiotics and claviridenone antineoplastics: (a) Smith, A. B., III; Branca, S. J.; Pilla, N. N.; Guaciaro, M. A. *J. Org. Chem.* **1982**, *47*, 1855. (b) Corey, E. J.; Mehrota, M. M. *J. Am. Chem. Soc.* **1984**, *106*, 3384. (c) Sugiura, S.; Hazato, A.; Tanaka, T.; Okamura, N.; Bannai, K.; Manabe, K.; Kurozumi, S.; Suzuki, M.; Noyori, R. *Chem. Pharm. Bull.* **1985**, *33*, 4120. (d) Iwasaki, G.; Sano, M.; Sodeoka, M.; Yoshida, K.; Shigasaki, M. *J. Org. Chem.* **1988**, *53*, 4864. (e) Iguchi, K.; Kaneta, S.; Nagaoka, H.; Yamada, Y. *Chem. Lett.* **1989**, *160*, 157.

(3) (a) Kollenz, G.; Ott, W.; Ziegler, E.; Peters, K.; von Schnering, H. G.; Quast, H. *Liebigs Ann. Chem.* **1980**, 1801. (b) Imming, P.; Mohr, R.; Mueller, E.; Overheu, W.; Seitz, G. *Angew. Chem., Int. Ed. Engl.* **1982**, *21*, 284. (c) Hussong, R.; Heydt, H.; Regitz, M. *Z. Naturforsch. B* **1986**, *41B*, 915. (d) Padwa, A.; Norman, B. H. *J. Org. Chem.* **1990**, *55*, 4801. (e) Curran, D. P.; Liu, H. *J. Am. Chem. Soc.* **1991**, *113*, 2127. (f) Rigby, J. H.; Qabar, M. *J. Am. Chem. Soc.* **1991**, *113*, 8975.

(4) (a) Trost, B. M.; Matelich, M. C. *J. Am. Chem. Soc.* **1991**, *113*, 9007. (b) Trost, B. M.; Grese, T. A.; Chan, D. M. *J. Am. Chem. Soc.* **1991**, *113*, 7350. (c) Boivin, J.; Tailhan, C.; Zard, S. Z. *J. Am. Chem. Soc.* **1991**, *113*, 5874. (d) Rathjen, H.-J.; Margaretha, P.; Wolff, S.; Agosta, W. C. *J. Am. Chem. Soc.* **1991**, *113*, 3904. (e) Trost, B. M. *Angew. Chem., Int. Ed. Engl.* **1986**, *25*, 1. (f) Danheiser, R. L.; Carini, D. J.; Fink, D. M.; Basak, A. *Tetrahedron* **1983**, *39*, 935. (g) Noyori, R. *Acc. Chem. Res.* **1979**, *12*, 61.

(5) (a) Pauson, P. L. *Organometallics in Organic Synthesis*; de Meijere, A., tom Dieck, H., Eds.; Springer-Verlag: Berlin, 1987; p 234. (b) Schore, N. E. *Chem. Rev.* **1988**, *88*, 1081. (c) Pauson, P. L. *Tetrahedron* **1985**, *41*, 5855. (d) Billington, D. C.; Pauson, P. L. *Organometallics* **1982**, *1*, 1560.

(6) Ruitenberg, K.; Kleijn, H.; Elsevier, C. J.; Meijer, J.; Vermeer, P. *Tetrahedron Lett.* **1981**, *22*, 1451.

(7) The supplementary material contains synthetic details, X-ray crystallographic analysis, and analytical data.

(8) Kleveland, K.; Skattebol, L. *Acta Chem. Scand. B* **1975**, *29*, 191.

(9) Jewell, C. F., Jr.; Liebeskind, L. S.; Williamson, M. *J. Am. Chem. Soc.* **1985**, *107*, 6715.

(10) Alcock, N. W.; Richards, C. J.; Thomas, S. E. *Organometallics* **1991**, *10*, 231.

(11) Eaton, B. E.; King, J. A., Jr.; Vollhardt, K. P. C. *J. Am. Chem. Soc.* **1986**, *108*, 1359.

(12) Faller, J. W.; Rosen, A. M. *J. Am. Chem. Soc.* **1977**, *99*, 4858.

(13) (a) Benn, R.; Schroth, G. *J. Organomet. Chem.* **1982**, *228*, 71. (b) Yasuda, H.; Tatsumi, K.; Nakamura, A. *Acc. Chem. Res.* **1985**, *18*, 120. (c) Erker, G.; Engel, K.; Kruger, C.; Tsay, Y.-H.; Samuel, E.; Vogel, P. *Z. Naturforsch. B* **1985**, *40B*, 150.